

Supplementary Information

Azo-carbazole copolymer-based composite films with high transparency for updatable holograms

Kenji Kinashi ^{a*}, Ikumi Nakanishi ^b, Wataru Sakai ^a, Naoto Tsutsumi ^a, Boaz Jessie Jackin ^c

- a. Faculty of Materials Science and Engineering, Kyoto Institute of Technology, Matsugasaki, Sakyo, Kyoto 606-8585, Japan.
- b. Master's Program of Innovative Materials, Graduate School of Science and Technology, Kyoto Institute of Technology, Matsugasaki, Sakyo, Kyoto 606-8585, Japan.
- c. Materials Innovation Laboratory, Kyoto Institute of Technology

Experimental

Diffraction efficiency was measured using a 4f reduction projection system, as shown in **Figure S1**. A vertical fringe pattern image with *s*-polarized 532 nm writing beam (500mW, Samba™, Cobolt Co.) reflected through a polarizing beam-splitter (PBS) were projected directly onto the film. A PC-controlled vertical fringe interference pattern with a grating number 100 on a special light modulator (SLM) (1920 pixels wide × 1080 pixel high; 8.0 μm pixel size, HOLOEYE Photonics Co.) gives fringe pattern spacing $\Lambda = 25 \mu\text{m}$ on the film surface. A weak *s*-polarized probing beam of 1 mW DPSS laser at 640 nm (500 mW, Bolero™, Cobolt Co.) illuminated on the film surface, and then a first-order (+1st order) diffraction intensity from the resultant refractive index gratings was measured by a silicon photodiode. An ITO transparent heater (SS-051, BLAST Co.) was used for measuring thermal stability of the first-order diffraction intensity.

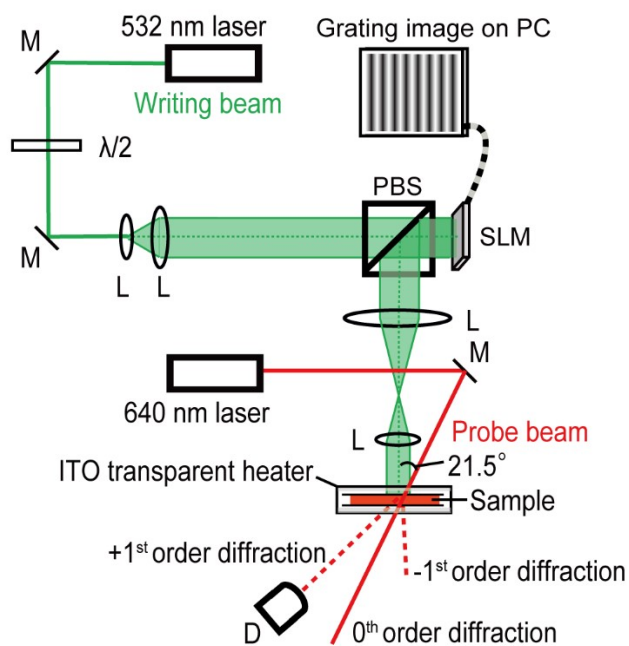


Figure S1 Schematic representation of the 4f reduction projection system: L, lens; M, mirror; $\lambda/2$, half-wave plate; PBS, polarizing beam splitter; PC, personal computer; SLM, spatial light modulator; D, photodiode. Laser sources are a green CW laser at 532 nm for writing and a red laser at 640 nm for probing.

Schematic apparatus for the updatable holographic imaging of the object is shown in **Figure S2**. One *s*-polarized 532 nm recording beam (500 mW, Samba™, Cobolt Co.) reflected by a polarizing beam-splitter (PBS) was magnified by an objective lens (40x) and another lens to illuminate an object, and the reflected object beam was projected directly onto the film. The other *s*-polarized beam was used as a reference beam and interfered with the objective beam on the film surface. A half-wave plate in front of the PBS was used to control the intensity ratio of the object and reference beams. The recorded holograms were simultaneously reconstructed by a *p*-polarized 642 nm reconstruction beam (140 mW, PhoxX 642, Omicron Co.) magnified by a pair of lenses. The reconstructed hologram image was erased using an ITO transparent heater (SS-051, BLAST Co.).

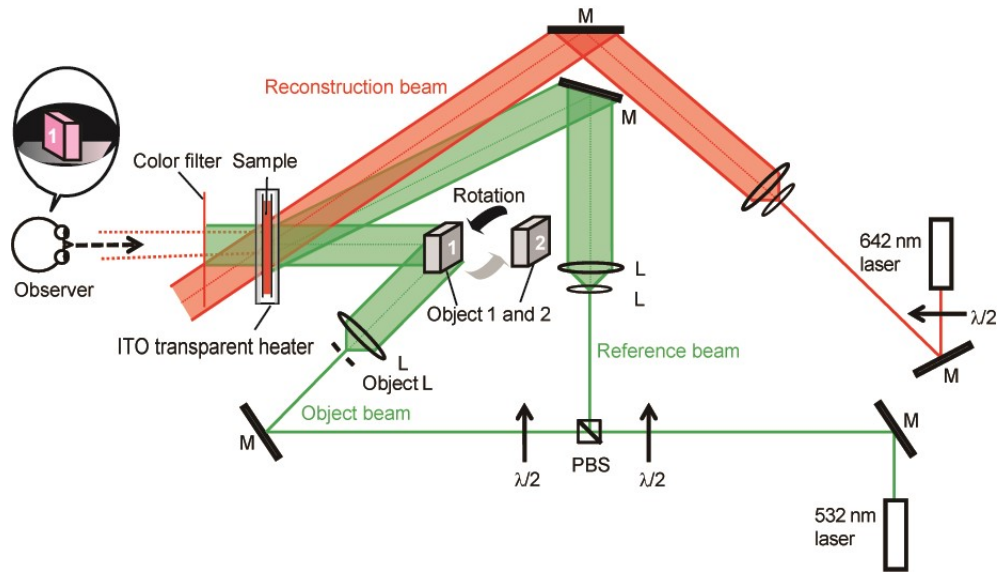


Figure S2 Schematic representation of the holographic display system: L, lens; M, mirror; $\lambda/2$, half-wave plate; PBS, polarizing beam splitter. Laser sources are a green CW laser at 532 nm for recording and a red laser at 642 nm for reconstructing.

The haze value was measured to evaluate the transparency and scattering properties of the samples using an integrating sphere (**Figure S3**). The haze value (%) was calculated by

$$\text{Haze value} = \frac{T_d}{T_t} \times 100,$$

where T_t is the total transmitted light intensity, and T_d is the scattered transmitted light.

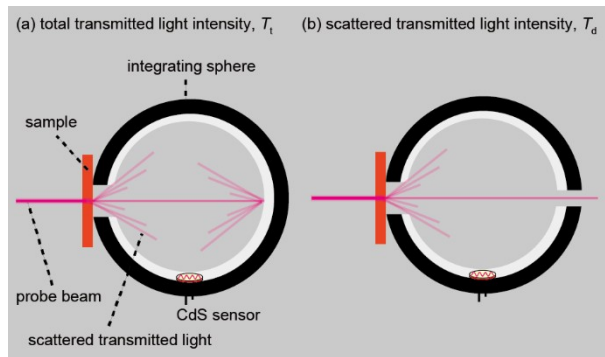


Figure S3. Haze value measurement system. (a) Measuring total transmitted light intensity. (b) Measuring scattered transmitted light intensity. A collimated light of 633 nm was used as the probe beam.

Table S1. Bessel functions of the first kind $J_n(\delta)$ and corresponding first-order diffraction efficiencies.

δ	$J_0(\delta)$	$J_1(\delta)$	$J_1^2(\delta)$	$\eta_1, \%$
0.0	1	0	0	0
0.1	0.99750	0.04994	0.00250	0.25
0.2	0.99002	0.09950	0.00990	0.99
0.3	0.97763	0.14832	0.02200	2.20
0.4	0.96040	0.19603	0.03840	3.84
0.5	0.93847	0.24227	0.05870	5.87
0.6	0.91200	0.28670	0.08220	8.22
0.7	0.88120	0.32900	0.10820	10.82
0.8	0.84629	0.36884	0.13600	13.60
0.9	0.80752	0.40595	0.16480	16.48
1.0	0.76520	0.44005	0.19360	19.36
1.1	0.71962	0.47090	0.22170	22.17
1.2	0.67113	0.49829	0.24830	24.83
1.3	0.62009	0.52202	0.27250	27.25
1.4	0.56686	0.54195	0.29370	29.37
1.5	0.51183	0.55794	0.31130	31.13
1.6	0.45540	0.56990	0.32480	32.48
1.7	0.39798	0.57777	0.33380	33.38
1.8	0.33999	0.58152	0.33820	33.82
1.9	0.28182	0.58116	0.33770	33.77
2.0	0.22389	0.57672	0.33260	33.26
2.1	0.16661	0.56829	0.32295	32.30
2.2	0.11036	0.55596	0.30909	30.91
2.3	0.05554	0.53987	0.29146	29.15
2.4	0.00251	0.52019	0.27060	27.06